Effects of a Moderate-Intensity Static Magnetic Field and Adriamycin on K562 Cells

Qi Hao,[1]* Chen Wenfang,[2] Ai Xia,[1] Wei Qiang,[1] Liu Ying,[2] Zhang Kun,[1] and Sun Runguang[2]

[1]*College of Life Science, Shaanxi Normal University, Xi'an, Shaanxi, P. R. China*
[2]*College of Physics and Information Technology, Shaanxi Normal University, Xi'an, Shaanxi, P. R. China*

The aim of this study was to investigate whether a moderate-intensity static magnetic field (SMF) can enhance the killing effect of adriamycin (ADM) on K562 cells, and to explore the effects of SMF combined with ADM on K562 cells. We analyzed the metabolic activity of cells, cell cycle distribution, DNA damage, change in cell ultrastructure, and P-glycoprotein (P-gp) expression after K562 cells were exposed continuously to a uniform 8.8 mT SMF for 12 h, with or without ADM. Our results showed that the SMF combined with ADM (25 ng/ml) significantly inhibited the metabolic activity of K562 cells ($P < 0.05$), while neither ADM nor the SMF alone affected the metabolic activity of these cells. Cell ultrastructure was altered in the SMF + ADM group. For example, cell membrane was depressed, some protuberances were observable, and vacuoles in the cytoplasm became larger. Cells were arrested at the G2/M phase and DNA damage increased after cells were treated with the SMF plus ADM. ADM also induced the P-gp expression. In contrast, in the SMF group and SMF + ADM group, the P-gp expression was decreased compared with the ADM group. Taken together, our results showed that the 8.8 mT SMF enhanced the cytotoxity potency of ADM on K562 cells, and the decrease in P-gp expression may be one reason underlying this effect. Bioelectromagnetics. © 2010 Wiley-Liss, Inc.

Key words: static magnetic field; killing effects; cell cycle; DNA damage; P-glycoprotein

INTRODUCTION

Adriamycin (ADM) is an anthracycline antitumor drug that has been widely used in the clinic for the treatment of various cancers [Samson et al., 1987; Krommer and Szalai, 1992]. The antitumor activity of ADM results from its interactions with DNA, which can inhibit both DNA replication and RNA transcription, or impair topoisomerase II activity [Meriwether and Bachur, 1972; Tewey et al., 1984]. However, drug resistance of cancer cells and side effects of ADM are major obstacles for a successful ADM therapy [Minotti et al., 2004].

Recently, some studies have suggested that static magnetic fields (SMFs) have the potential as an adjunctive treatment method for chemotherapy, since SMFs influence cell growth, proliferation, and cell structure of cancer cells [Raylman et al., 1996; Chionna et al., 2005; Brix et al., 2008; Strieth et al., 2008; Strelczyk et al., 2009; Feng et al., 2010; Hsu and Chang, 2010; Kim and Im, 2010; Martino et al., 2010; Yang et al., 2010]. In particular, the killing effect of antineoplastic drugs on cancer cells is enhanced with a combined treatment of SMFs and chemotherapeutic drugs, indicating that SMFs act synergically with the pharmacological treatment [Gray et al., 2000; Sabo et al., 2002; Tofani et al., 2003]. For example, 64 h exposure to a 7 Tesla uniform SMF produced a reduction in viable cell number in HTB 63 (melanoma), HTB 77 IP3 (ovarian carcinoma), and CCL 86 (lymphoma, Raji cells) cell lines [Raylman et al., 1996]. Gray et al. [2000] evaluated the effects of non-uniform 110 mT SMF for four 4 h periods, with 8–12 h between each exposure, and doxorubicin (10 mg/kg, i.p.) on female B6C3F1 mice with transplanted mammary adenocarcinoma. Their results revealed that the groups exposed to SMF combined with doxorubicin achieved significantly greater tumor regression than the group treated with ADM alone. In an in vitro cell growth assay, the application of 1 T SMF for 72 h on HL-60 cells,

The authors declare that they have no competing interests.

Grant sponsors: National Natural Science Foundation of China (20772077); National Basic Research Priority Program of China (104167); Fundamental Research for the Central Universities (GK200902033).

*Correspondence to: Qi Hao, College of Life Science, Shaanxi Normal University, 199 South Chang'an Road, Xi'an 710062, Shaanxi, P. R. China. E-mail: qhsnnu@126.com

Received for review 1 April 2010; Accepted 22 September 2010

DOI 10.1002/bem.20625
Published online in Wiley Online Library (wileyonlinelibrary.com).

combined with a mixture of antineoplastic drugs (5-fluorouracil, cisplatin, doxorubicin, and vincristine), enhanced the cytotoxic effect of antineoplastic drugs [Sabo et al., 2002]. In an in vivo experiment, mice bearing murine Lewis lung carcinomas (LLCs) were treated with 3 mT SMF for 35 min/day and cisplatin (3 mg/kg, i.p.) [Tofani et al., 2003]. The survival time of mice treated with cisplatin and SMF was significantly longer than that of mice treated only with cisplatin or SMF exposure. These results show that SMF can inhibit the proliferation of cancer cells, and the killing effects of SMF combined with antineoplastic drugs on cancer cells are greater than those of SMFs or anticancer drugs alone. These observations suggest a potential strategy for chemotherapy, that is, the combination therapy of SMFs and chemotherapeutic drugs. However, so far it remains unclear which mechanism underlies the killing effects of SMFs combined with chemotherapy drugs on cancer cells.

Therefore, we aimed to examine the killing effects of SMFs coupled with ADM on K562 cells, and to explore the interrelationship between SMFs and ADM on cell activity, cell ultrastructure, cell cycle distribution, and DNA damage of K562 cells. We chose K562 cells as the model because multidrug resistance (MDR) can be easily induced by ADM, resulting from the overexpression of the MDR-1 gene product, P-glycoprotein (P-gp) [Hamada and Tsuruo, 1988]. Next, we investigated the P-gp expression of K562 cells exposed to ADM, with or without SMF, in order to understand the mechanism of the killing effects of SMF and ADM.

MATERIALS AND METHODS

Cell Cultures

K562 cells (ATCC, CCL-243) were obtained from the cell bank of the Type Culture Collection of the Chinese Academy of Sciences (320 Yue Yang Road, Shanghai, China). They were grown at 37 °C in an atmosphere containing 5% CO_2 and with a relative humidity of 100%. The culture medium used was RPMI-1640 (Sigma–Aldrich, St. Louis, MO), supplemented with 10% fetal bovine serum (Gibco-Invitrogen, Grand Island, NY), and 1 mM L-glutamine (Sigma–Aldrich). Logarithmic phase cells were used for the experiments.

Magnetic Field Application

The SMF was produced by a solenoid provided by the College of Physics and Information Technology, Shaanxi Normal University, Shaanxi, China. The SMF was made of copper wire wound around a ring former with a radius of 4 cm and length of 54.7 cm. The solenoid was set on supports made of non-magnetic material that had maximal thermal and mechanical stability, suitable for operations extending over several weeks. The power source was a direct current power supply with an accuracy of 0.5% at 50 ± 5 Hz (WYJ, Shanghai, China). This device produced a homogeneous SMF in a volume close to the axis with a calculated magnetic flux intensity of 9 mT. A gauss meter (HT20, Hengtong Magnetoelectricity, Shanghai, China) measured the actual value of the magnetic flux intensity at 8.800 ± 0.106 mT. The water flow from a cooling bath was circulated through a tube surrounding the solenoid to disperse the Joule effect. A non-magnetic and airtight incubator (length 25 cm, width 5 cm, and height 5 cm) was used to place the samples within the middle of the solenoid. The samples were placed on the bottom of the incubator. The temperature in the incubator was monitored by a heater and a thermo-controller to keep the incubator temperature constant at 36.5 ± 0.5 °C. Then, 32 ml of CO_2 was insufflated into the incubator to maintain the pH of the medium between 7.2 and 7.4. The CO_2 concentration was measured using a handheld CO_2 concentration measurement net adapter (InControl 1050, Dräger, Luebeck, Germany), and a measurement system that could maintain the CO_2 concentration for at least 40 h. Pre-testing results showed that the proliferation of cells was similar in both incubators ($P > 0.05$). Figure 1 shows the exposure position and magnetic flux density at the floor level of the incubator. For the sham-exposure system, a unit with the same coil shape was used, but without the SMF generator.

Considering that the cell cycle of K562 cells is 12 h [Lozzio and Lozzio, 1975], multiples of 12 h were chosen as the exposure time at different magnetic flux densities (3–15 mT) in pre-experiments. Fortunately, the exposure time at which SMF inhibited the proliferation of K562 cells was twice that of the cell cycle time at 8.8 mT. Therefore, we chose 8.8 mT as the magnetic flux density for our experiments.

Experimental Groups

Logarithmically growing K562 cells were inoculated in cell culture bottles at a density of 1×10^5 cells/ml and randomly divided into four groups: (1) control group, in which all conditions were the same, except for the SMF treatment, (2) SMF group, in which cells were continuously exposed to the SMF for 12 h, (3) ADM group, in which cells were incubated with different concentrations of ADM (25, 35, and 50 ng/ml) for 12 h, and (4) SMF + ADM group, with the combined SMF and ADM treatment as described above.

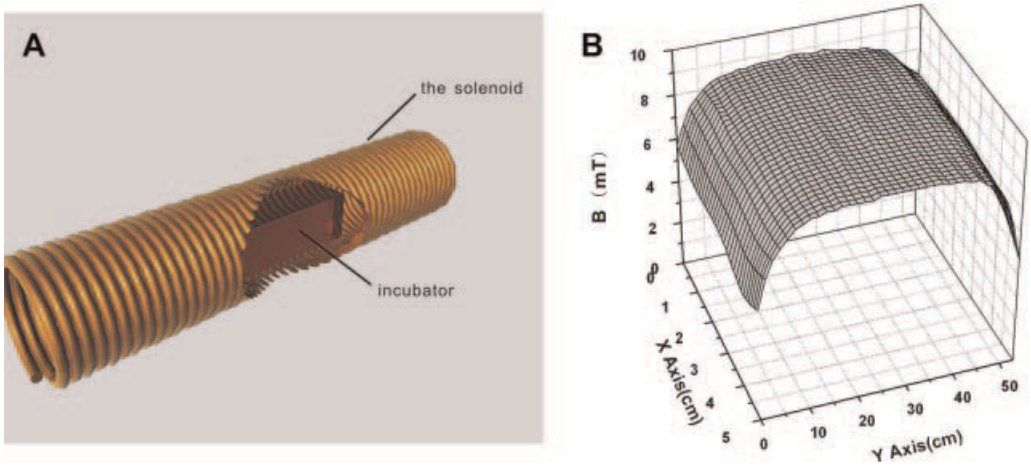

Fig. 1. **A**: Sketch of the static magnetic field (SMF) exposure system. A non-magnetic and airtight incubator was used to hold the samples placed within the middle of solenoid. **B**: Distribution of magnetic flux density, measured along the center axis at the floor level of the cell culture bottles. The *X*-direction is the width of the incubator and the *Y*-direction is the length of the solenoid.

MTT Assay

The 3-(4,5-dimethylthiazol-2-yl)-2,5-diphenyltetrazolium bromide (MTT) assay was performed as previously described [Mosmann, 1983]. Briefly, cell suspensions were cultivated in 96-well cell culture clusters (Corning, Lowell, MA) at a final volume of 100 μL. Concomitantly, 10 μl MTT (1 mg/ml, Sigma–Aldrich) was added to each sample. The cultivation was performed at 37 °C in a humidified 5% CO_2 atmosphere for 4 h. During this period, the living cells produced a blue, insoluble formazan product. The metabolic activity of cells was directly associated with the amount of formazan produced. After solubilization of the crystals in 0.2 ml of dimethyl sulfoxide (DMSO) per well, the optical density (OD) was obtained at 570 nm using a microplate reader (Model 680, Bio-Rad Laboratories, Irvine, CA). Each group contained 6–8 wells and the experiments were performed at least three times.

Atomic Force Microscopic Observation

The atomic force microscope (AFM) used was an SPM-9500J3 with WET CNII (Shimadzu, Kyoto, Japan) that operated in air. A V-shaped, Si_3N_4 cantilever (OMCL-TR800PSA-1, Olympus, Tokyo, Japan) with a 0.12 N/m spring constant was used in the experiment. During the experiment, the scan rate was adjusted between 1.0 and 1.5 Hz in contact mode. The obtained images were processed by custom software.

According to the modified protocol by Zhuang et al. [2005] for cell samples, cells were gently rinsed twice with phosphate-buffered saline (PBS, pH 7.2, 0.1 M). The cells were fixed by 1% glutaraldehyde for 15 min and then gently rinsed with PBS (pH 7.2, 0.1 M) twice. The cell density was adjusted to 1×10^6 cells/ml. The cell suspension was dropped onto the surface of freshly cleaved mica (the size of mica was fitted to the size of the sample holder). After airing, the mica was mounted on the AFM stage and observed with the contact mode of the AFM in the atmosphere.

Transmission Electron Microscopic Observation

Transmission electron microscopic (TEM) analyses of K562 cells were performed as previously described [Liu et al., 2003]. After treatment, the cells were rinsed, pelletized, and then resuspended in 0.1 M phosphate buffer (pH 7.3) containing 1% (v/v) glutaraldehyde at 4 °C for 2 h. The cells were rinsed three times in 0.1 M phosphate buffer for 10 min each time. Post-fixation was carried out with 1% (w/v) osmium tetroxide prepared in 0.1 M phosphate buffer for 1–2 h at room temperature. The cells were then dehydrated with 50% (v/v) ethanol for 15 min, followed by 75% (v/v) ethanol for 15 min, 95% (v/v) ethanol for 15 min twice, 100% (v/v) ethanol for 15 min twice, and finally 100% (v/v) acetone for 20 min. Infiltration was conducted with a mixture of acetone and Epon 812 in ratios of 3:1, 1:1, and 1:3 for 1 h. Then, Epon 812 was infiltrated for 24–48 h. Subsequently, the cells were embedded and polymerized at 60 °C for 24–48 h, sectioned with ultramicrotome, and stained with uranyl acetate and lead citrate. The samples were examined and observed under a Hitachi H-600 TEM (Tokyo, Japan).

Cell Cycle Distribution Analysis

Cells were harvested by centrifugation, washed with PBS, and fixed overnight in 70% ethanol at 4 °C.

The samples were stained with a DNA-Prep reagents kit (Beckman Counter, Fullerton, CA) in darkness for 25 min at 25 °C and detected using flow cytometry (FACSCalibur, Becton Dickinson, Franklin Lakes, NJ). The data from 20000 cells was analyzed using ModFit LT 3.0 for Mac software (Verity House, Topsham, ME) that was designed for this apparatus.

Comet Assay

Before the experiment, slides were coated with 0.2% agarose. A clean cover slip was placed on the slide to build a 22 mm × 10 mm × 0.17 mm small gap. After K562 cells were treated with SMF and/or ADM, cells were collected by centrifugation (400*g*, 3 min), and the cell density was adjusted to 3×10^5 cells/ml with PBS. According to the modified comet assay protocol [Luo et al., 2006], approximately 3×10^4 cells in 0.1 ml PBS were mixed with 0.1 ml of 1% low-melting-point agarose (Sigma–Aldrich). The mixture was placed in the above-mentioned gap. The cover glasses were carefully removed after the agarose layer was solidified. The layer was treated with lysis buffer (2.5 M NaCl, 100 mM EDTA, 10 mM Tris, 200 mM NaOH, 1% *N*-lauroyl-sarcosine, pH 10; 1% Triton, and 10% DMSO were added immediately before use) for 60 min at 4 °C. After the cells were lysed, the slides were washed three times in triple-distilled water at 4 °C. The lysed cells were then placed in an electrophoresis chamber, exposed to alkali (300 mM NaOH, 1 mM EDTA, pH 13) for 20 min at 4 °C, and electrophoresed for 20 min at 0.86 V/cm and 4 °C. After electrophoresis, the slides were washed three times with 0.4 M Tris–HCl (pH 7.4) at 4 °C. The slides were subsequently dried with 90% and 100% ethanol, stained with ethidium bromide (20 μg/ml, Sigma–Aldrich) and imaged with a fluorescent microscope (E600, Nikon, Sendai, Japan) with a digital sight (DS-SMC, Nikon). The image analysis was performed using Comet Assay Software Project (CASP) freeware (University of Wroclaw, Poland) [Hellman et al., 1995; Helma and Uhl, 2000; Bowden et al., 2003; Konca et al., 2003]. In each experimental group, 150 cells were evaluated from three different slides and the cellular DNA damage was calculated based on olive tail moment (OTM) visualization. The experiment was performed at least three times.

Analysis of P-Glycoprotein Expression Using Flow Cytometry

Analysis of P-gp expression using flow cytometry was performed according to a method described by Guerci et al. [1995]. Briefly, cells were harvested by centrifugation (100*g*, 5 min) and washed with PBS. After 4% polyformaldehyde was added for 20 min at 4 °C, the cells were permeabilized with 3% methanol for 10 min, blocked with 5% goat serum (Zhongshan Goldenbridge Biotechnology, Beijing, China) for 1 h at 37 °C, and incubated with a mouse monoclonal antibody, MDR Ab-2 (clone F4, 1:100, Thermo Fisher Scientific, Fremont, CA) for 1 h at room temperature. After washing, the cells were stained with fluorescein isothiocyanate (FITC)-labeled goat anti-mouse IgG_1 antibody (1:100, Zhongshan Goldenbridge Biotechnology) and detected using flow cytometry. The analysis was based on acquisition of data from 10000 cells using ModFit LT 3.0 for Mac software.

Statistical Analysis

Statistical analyses were performed using ANOVA and the Mann–Whitney *U*-test with a minimal confidence level of 0.05 for statistical significance. Each experiment was performed at least three times.

RESULTS

Inhibition Effect of SMF and ADM on Cell Proliferation

Pre-testing results showed that cell proliferation was significantly inhibited by a 24 h exposure to SMF ($P < 0.05$) or a 12 h incubation with 35 ng/ml ADM ($P < 0.05$) when K562 cells were seeded at a density of 1×10^5 cells/ml (data not shown).

Figure 2 shows the change in cell proliferation after K562 cells were treated with the SMF, with or without ADM. There was no significant difference between the ADM and control groups ($P > 0.05$) when the concentration of ADM was 25 ng/ml, while the cell proliferation of the SMF + ADM group was significantly reduced compared with the other three groups ($P < 0.01$). With an increase in the concentration of ADM, the killing effects of SMF combined with ADM became more obvious. These results suggested that the combined treatment of the SMF and the antineoplastic drug, ADM, significantly inhibited the cell proliferation of K562 cells, and the SMF enhanced the cytotoxic effect of ADM on K562 cells.

Fine Structure of Cell Surface and Combined Treatment of K562 Cells With SMF and ADM

Figure 3 shows the change in the cell surface ultrastructure observed by an AFM after K562 cells were treated with the SMF and ADM (25 ng/ml) for 12 h. The cell surface of controls was smooth and had a few minor folds (C in Fig. 3). When K562 cells were exposed to the SMF for 12 h, holes appeared in the cell surface (SMF in Fig. 3). The cell surface became rough, and the minor folds disappeared after K562 cells were

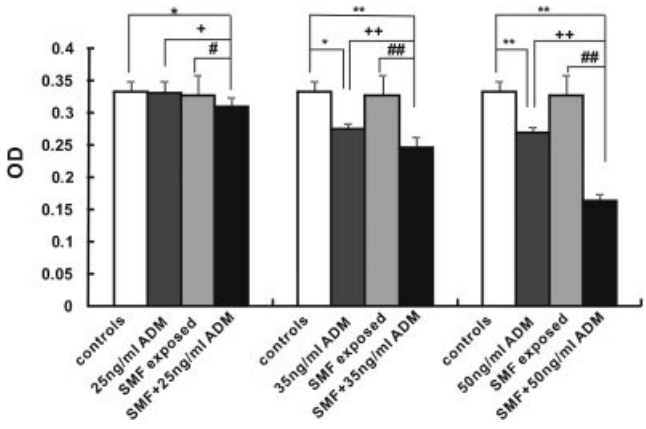

Fig. 2. Effect of 8.8 mT SMF coupled with ADM on the metabolic activity of K562 cells. Bars represent mean ± SD; $n = 6$. $^{*}P < 0.05$, $^{**}P < 0.01$ compared with controls; $++$ $P < 0.01$ compared with SMF; $\#\#$ $P < 0.01$ compared with ADM.

incubated in a concentration of 25 ng/ml ADM for 12 h (ADM in Fig. 3). In the SMF + ADM group, the holes and apophyses increased on the cell surface (SMF + ADM in Fig. 3). These results showed that the cell membrane damage in the SMF + ADM group was larger than the SMF group or the ADM group.

Cell Organelle Ultrastructure of Combined Treatment of K562 Cells With SMF and ADM

Figure 4 shows the change in the cell organelle ultrastructure observed by a TEM after K562 cells were treated with the SMF combined with ADM (25 ng/ml) for 12 h. In controls, the cell membrane was integrated, vacuoles in the cytoplasm were observed occasionally, and the cell nuclear membrane was integrated (C in Fig. 4). After cells were exposed to the SMF for 12 h, cystidiform structures with high electron density in the cytoplasm were increased. Other structures showed no

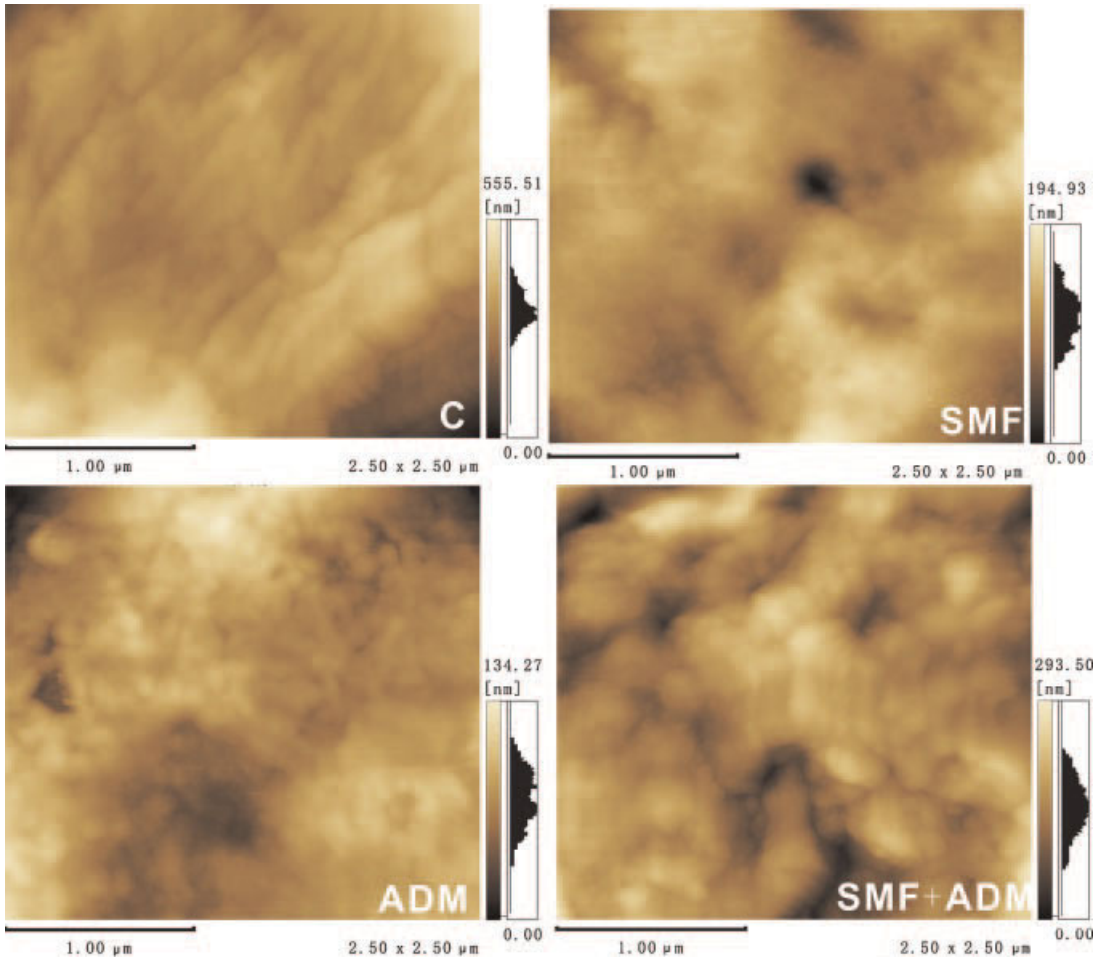

Fig. 3. Effect of 8.8 mT SMF combined with ADM on the fine structure of the K562 cell surface. The small black and white histogram on the right side of each image represents the height distribution of the cell surface. The color palette on the left of the histogram presents the relative height by different colors in the image. C, Controls; SMF, SMF-exposure group; ADM, 25 ng/ml ADM group; SMF + ADM, SMF combined with ADM (25 ng/ml).

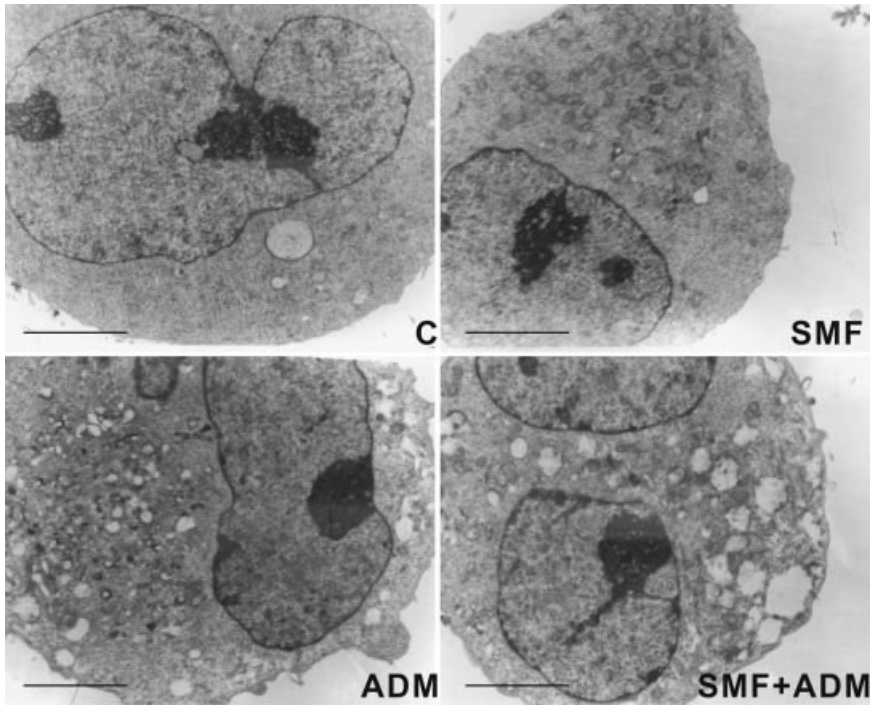

Fig. 4. Effect of 8.8 mT SMF combined with ADM on cell organelle ultrastructure of K562 cells. C, Controls; SMF, SMF-exposure group; ADM, 25 ng/ml ADM group; SMF + ADM, SMF combined with ADM (25 ng/ml). The bars represent 5 μm.

significant difference compared with controls (SMF in Fig. 4). In the ADM group, different-sized vacuoles in the cytoplasm were obviously increased, and a few strongly stained granules were randomly distributed in the cytoplasm (ADM in Fig. 4). The vacuole size in the cytoplasm was magnified during the 12 h exposure by the combination of SMF and ADM (SMF + ADM in Fig. 4). These data indicated that the killing effects on K562 cells were enhanced by the combined treatment of SMF and ADM.

Effect of the SMF and ADM Combination on Cell Cycle Distribution of K562 Cells

K562 cells were exposed to the SMF with or without 25 ng/ml ADM for 12 h, and the cell cycle distribution (Fig. 5A) and DNA damage (Fig. 5B) were subsequently analyzed using flow cytometry and comet assay. After exposure to the SMF for 12 h, the G2/M phase cell ratio was significantly increased compared with controls ($P < 0.05$) and the ratio of cells in the S phase was significantly lower than controls ($P < 0.05$), while the ratio of cells in the G1 phase was slightly but not significantly increased. The ADM treatment significantly increased the ratio of cells in the G2/M phase ($P < 0.05$) and significantly reduced the ratio of cells in the S phase compared with controls ($P < 0.01$). In the SMF + ADM group, the ratio of cells in the G2/M phase was increased, there were significant differences between the other three groups ($P < 0.05$ or <0.01), and the proportion of cells in the S phase was significantly reduced compared with controls ($P < 0.01$) or the SMF group ($P < 0.05$); however, there was no difference in the ADM group ($P > 0.05$).

OTM was used as the parameter to quantify the extent of cellular DNA damage when K562 cells were exposed to ADM with or without the SMF for 12 h (Fig. 5B). The experimental data showed that OTM of the SMF + ADM group was significantly higher than that of the other three groups ($P < 0.05$ or <0.01) when K562 cells were incubated with 25 ng/ml ADM with or without the SMF for 12 h. From these observations, we inferred that K562 cells treated with SMF and ADM were arrested in the G2/M phase due to DNA damage.

Effect of SMF Combined With ADM on P-Glycoprotein of K562 Cells

Figure 6 shows the proportion of P-gp expression in K562 cells that were exposed to the SMF and/or ADM for 12 h. When K562 cells were exposed to the SMF for 12 h, the ratio of P-gp expression was slightly but not significantly reduced compared with controls (SMF in Fig. 6). The ADM treatment induced the expression of P-gp in K562 cells, but there is no difference between controls and the ADM group (ADM

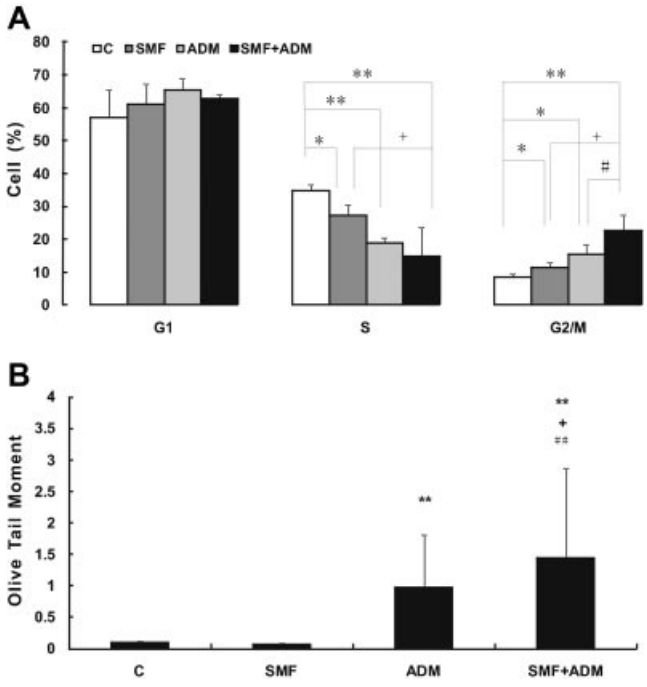

Fig. 5. K562 cells treated with SMF and 25 ng/ml ADM for 12 h. **A**: Distribution of the cell cycle in K562 cells exposed to 8.8 mT SMF with or without 25 ng/ml ADM. Bars represent mean ± SD; $n = 4$. $^{*}P < 0.05$, $^{**}P < 0.01$ compared with controls; $+$ $P < 0.05$ compared with SMF; $\#$ $P < 0.05$ compared with ADM. **B**: DNA damage was detected by the comet assay. Olive tail moment was used as the parameters to describe the extent of cellular DNA damage. Bars represent mean ± SD; $n = 150$. $^{**}P < 0.01$, compared with controls; $++$ $P < 0.01$ compared with SMF; $\#$ $P < 0.05$ compared with ADM.

in Fig. 6). In the combined treatment of SMF and ADM (SMF + ADM in Fig. 6), the ratio of K562 cells with P-gp expression was significantly reduced compared with the ADM group ($P < 0.01$), but there was no difference compared with controls ($P > 0.05$). These results showed that the SMF significantly inhibited the expression of P-gp induced by ADM; namely, the treatment of SMF plus ADM partially reversed the expression of P-gp induced by ADM.

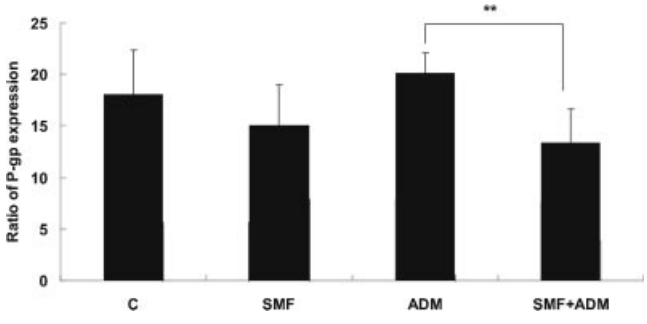

Fig. 6. Effects of 8.8 mT SMF combined with ADM on P-glycoprotein (P-gp) expression of K562 cells. Bars represent mean ± SD; $n = 6$. $^{**}P < 0.01$ compared with ADM.

DISCUSSION

In this study, we reported the in vitro biological effects of a uniform 8.8 mT SMF and ADM on human myelogenous leukemia K562 cells. We found that the SMF and ADM imposed a strong and replicable effect on the metabolic activity of cells, cell surface and inner ultrastructure modifications, and cell cycle distribution of K562 cells. Our study provided valuable evidence for changes in cell proliferation, surface fine structure, cell inner organelles, cell cycle distribution, and DNA damage. Meanwhile, we also examined the P-gp expression.

Several studies have reported the change in the metabolic activity of cells as a consequence of exposure to SMFs or electromagnetic fields (EMFs) combined with anticancer drugs in other cell lines [Raylman et al., 1996; Chakkalakal et al., 1999; Sabo et al., 2002; Tofani et al., 2003]. These studies and the present study suggest that the treatment of SMF plus antineoplastic drugs produces a synergetic killing effect on cancer cells.

An increasing number of studies evaluated the abilities of both SMF and EMF to enhance the in vivo or in vitro activity of a chemotherapeutic agent, but only a few of them have focused on various bio-effects. Gray et al. [2000] reported that the static field (static electric and SMFs) and ADM groups achieved significantly greater tumor regression than those with ADM only. Sabo et al. [2002] reported a metabolic activity retardation effect in the presence of SMF plus a mixture of the antineoplastic drugs (5-fluorouracil, cisplatin, doxorubicin, and vincristine). However, our data showed that when K562 cells were exposed to the SMF and ADM, cell surface and inner ultrastructure were injured, and the cell cycle was blocked at the G2/M phase. Previous studies reported similar results in other cell types or with other field types and intensities [Chionna et al., 2003, 2005; Tenuzzo et al., 2006]. Morphological modifications and the variations of the cell cycle distribution may be considered a common stress upon exposure to SMF and ADM, regardless of cell type and species. Interestingly, vesicle-like structures with high electron density, similar to organelles, were increased in K562 cells exposed to the SMF, suggesting that SMFs promoted the differentiation of K562 cells [Manni et al., 2004; Lisi et al., 2006; Sun et al., 2009].

We used an alkaline comet assay to assess DNA damage after exposure of K562 cells to 8.8 mT SMF and ADM for 12 h; this assay can detect DNA strand breaks with a high sensitivity [Olive et al., 1992]. Our results

showed that DNA lesions were significantly increased when K562 cells were treated by ADM with or without the SMF, but there was no detectable damage in the DNA of the SMF group. Considering that the ADM interactions with DNA can inhibit both DNA replication and RNA transcription [Meriwether and Bachur, 1972; Tewey et al., 1984], we considered that the lesions in DNA mainly resulted from ADM, and the SMF enhanced the cytotoxicity of ADM on K562 cells. Moreover, the role of ADM-induced free radicals and the concentration of free radicals in different exposure conditions has been described elsewhere [Rajagopalan et al., 1988; Jajte et al., 2002; Okano, 2008]. The role of oxygen free radicals in the cellular DNA lesions induced by SMF combined with ADM is worthy of further investigation.

K562 cells are characterized by multidrug resistance. Under the condition of anticancer drugs (e.g., ADM), K562 cells can easily produce P-gp [Hamada and Tsuruo, 1988]. P-gp is a transmembrane glycoprotein, and it functions as an adenosine 5′-triphosphate (ATP)-dependent drug transporter that unilaterally transports intracellular drugs out of the cells to acquire drug resistance [Gottesman et al., 2002; Teodori et al., 2006; Sauna and Ambudkar, 2007]. Increase in P-gp activity or expression induction leads to both a lowered intracellular accumulation and an increased efflux of drugs. In our study, an increase in the P-gp expression of K562 cells incubated with ADM was consistent with a previous study [Hamada and Tsuruo, 1988]. P-gp expression was slightly but not significantly decreased in the SMF-exposed cells compared with controls. However, the expression of P-gp in K562 cells exposed to SMF and ADM was significantly lower than that of cells exposed to ADM alone, suggesting that SMFs significantly inhibited the ADM-induced P-gp expression. Decreasing the induction of P-gp expression results in a higher intracellular accumulation and a decreased efflux of drugs. Thus, the inhibitory effect of SMFs on ADM-induced P-gp expression may be one of the reasons why SMFs synergize the killing effects of ADM on K562 cells.

REFERENCES

Bowden RD, Buckwalter MR, McBride JF, Johnson DA, Murray BK, O'Neill KL. 2003. Tail profile: A more accurate system for analyzing DNA damage using the Comet assay. Mutat Res 537(1):1–9.

Brix G, Strieth S, Strelczyk D, Dellian M, Griebel J, Eichhorn ME, Andrā W, Bellemann ME. 2008. Static magnetic fields affect capillary flow of red blood cells in striated skin muscle. Microcirculation 15(1):15–26.

Chakkalakal DA, Mollner TJ, Bogard MR, Fritz ED, Novak JR, McGuire MH. 1999. Magnetic field induced inhibition of human osteosarcoma cells treated with adriamycin. Cancer Biochem Biophys 17(1–2):89–98.

Chionna A, Dwikat M, Panzarini E, Tenuzzo B, Carla EC, Verri T, Pagliara P, Abbro L, Dini L. 2003. Cell shape and plasma membrane alterations after static magnetic fields exposure. Eur J Histochem 47(4):299–308.

Chionna A, Tenuzzo B, Panzarini E, Dwikat MB, Abbro L, Dini L. 2005. Time dependent modifications of Hep G2 cells during exposure to static magnetic fields. Bioelectromagnetics 26(4):275–286.

Feng SW, Lo YJ, Chang WJ, Lin CT, Lee SY, Abiko Y, Huang HM. 2010. Static magnetic field exposure promotes differentiation of osteoblastic cells grown on the surface of a poly-L-lactide substrate. Med Biol Eng Comput 48(8):793–798.

Gottesman MM, Fojo T, Bates SE. 2002. Multidrug resistance in cancer: Role of ATP-dependent transporters. Nat Rev Cancer 2(1):48–58.

Gray JR, Frith CH, Parker JD. 2000. In vivo enhancement of chemotherapy with static electric or magnetic fields. Bioelectromagnetics 21(8):575–583.

Guerci A, Merlin JL, Missoum N, Feldmann L, Marchal S, Witz F, Rose C, Guerci O. 1995. Predictive value for treatment outcome in acute myeloid leukemia of cellular daunorubicin accumulation and P-glycoprotein expression simultaneously determined by flow cytometry. Blood 85(8):2147–2153.

Hamada H, Tsuruo T. 1988. Characterization of the ATPase activity of the Mr 170,000 to 180,000 membrane glycoprotein (P-glycoprotein) associated with multidrug resistance in K562/ADM cells. Cancer Res 48(17):4926–4932.

Hellman B, Vaghef H, Bostrom B. 1995. The concepts of tail moment and tail inertia in the single cell gel electrophoresis assay. Mutat Res 336(2):123–131.

Helma C, Uhl M. 2000. A public domain image-analysis program for the single-cell gel-electrophoresis (comet) assay. Mutat Res 466(1):9–15.

Hsu SH, Chang JC. 2010. The static magnetic field accelerates the osteogenic differentiation and mineralization of dental pulp cells. Cytotechnology 62(2):143–155.

Jajte J, Grzegorczyk J, Zmyslony M, Rajkowska E. 2002. Effect of 7 mT static magnetic field and iron ions on rat lymphocytes: Apoptosis, necrosis and free radical processes. Bioelectrochemistry 57(2):107–111.

Kim S, Im W. 2010. Static magnetic fields inhibit proliferation and disperse subcellular localization of gamma complex protein3 in cultured C2C12 myoblast cells. Cell Biochem Biophys 57(1):1–8.

Konca K, Lankoff A, Banasik A, Lisowska H, Kuszewski T, Gozdz S, Koza Z, Wojcik A. 2003. A cross-platform public domain PC image-analysis program for the comet assay. Mutat Res 534(1–2):15–20.

Krommer CF, Szalai JP. 1992. Cyclophosphamide, adriamycin and cisplatin (CAP) versus cyclophosphamide, adriamycin and vincristin (CAV) in the treatment of advanced ovarian cancer: A randomized study. Ann Oncol 3(1):37–39.

Lisi A, Ledda M, Rosola E, Pozzi D, D'Emilia E, Giuliani L, Foletti A, Modesti A, Morris SJ, Grimaldi S. 2006. Extremely low frequency electromagnetic field exposure promotes differentiation of pituitary corticotrope-derived AtT20 D16V cells. Bioelectromagnetics 27(8):641–651.

Liu Q, Sun S, Xiao Y, Qi H, Shang Z, Zhang J, Ren Y, Li M, Li Q. 2003. Study of cell killing and morphology on S180 by ultrasound activating hematoporphyrin derivatives. Sci China C Life Sci 46(3):253–262.

Lozzio CB, Lozzio BB. 1975. Human chronic myelogenous leukemia cell-line with positive Philadelphia chromosome. Blood 45(3):321–334.

Luo M, Qi H, Chen W, Liu M, Guo W. 2006. DNA damage induced by UV in K562 cells measured by comet assay. Carcinog Teratog Mutagen 18(5):400–403.

Manni V, Lisi A, Rieti S, Serafino A, Ledda M, Giuliani L, Sacco D, D'Emilia E, Grimaldi S. 2004. Low electromagnetic field (50 Hz) induces differentiation on primary human oral keratinocytes (HOK). Bioelectromagnetics 25(2):118–126.

Martino CF, Perea H, Hopfner U, Ferguson VL, Wintermantel E. 2010. Effects of weak static magnetic fields on endothelial cells. Bioelectromagnetics 31(4):296–301.

Meriwether WD, Bachur NR. 1972. Inhibition of DNA and RNA metabolism by daunorubicin and adriamycin in L1210 mouse leukemia. Cancer Res 32(6):1137–1142.

Minotti G, Menna P, Salvatorelli E, Cairo G, Gianni L. 2004. Anthracyclines: Molecular advances and pharmacologic developments in antitumor activity and cardiotoxicity. Pharmacol Rev 56(2):185–229.

Mosmann T. 1983. Rapid colorimetric assay for cellular growth and survival: Application to proliferation and cytotoxicity assays. J Immunol Methods 65(1–2):55–63.

Okano H. 2008. Effects of static magnetic fields in biology: Role of free radicals. Front Biosci 13:6106–6125.

Olive PL, Wlodek D, Durand RE, Banath JP. 1992. Factors influencing DNA migration from individual cells subjected to gel electrophoresis. Exp Cell Res 198(2):259–267.

Rajagopalan S, Politi PM, Sinha BK, Myers CE. 1988. Adriamycin-induced free radical formation in the perfused rat heart: Implications for cardiotoxicity. Cancer Res 48:4766–4769.

Raylman RR, Clavo AC, Wahl RL. 1996. Exposure to strong static magnetic field slows the growth of human cancer cells in vitro. Bioelectromagnetics 17(5):358–363.

Sabo J, Mirossay L, Horovcak L, Sarissky M, Mirossay A, Mojzis J. 2002. Effects of static magnetic field on human leukemic cell line HL-60. Bioelectrochemistry 56(1–2):227–231.

Samson MK, Wasser LP, Borden EC, Wanebo HJ, Creech RH, Phillips M, Baker LH. 1987. Randomized comparison of cyclophosphamide, imidazole carboxamide, and adriamycin versus cyclophosphamide and adriamycin in patients with advanced stage malignant mesothelioma: A Sarcoma Intergroup Study. J Clin Oncol 5(1):86–91.

Sauna ZE, Ambudkar SV. 2007. About a switch: How P-glycoprotein (ABCB1) harnesses the energy of ATP binding and hydrolysis to do mechanical work. Mol Cancer Ther 6(1):13–23.

Strelczyk D, Eichhorn ME, Luedemann S, Brix G, Dellian M, Berghaus A, Strieth S. 2009. Static magnetic fields impair angiogenesis and growth of solid tumors in vivo. Cancer Biol Ther 8(18):1756–1762.

Strieth S, Strelczyk D, Eichhorn ME, Dellian M, Luedemann S, Griebel J, Bellemann M, Berghaus A, Brix G. 2008. Static magnetic fields induce blood flow decrease and platelet adherence in tumor microvessels. Cancer Biol Ther 7(6):814–819.

Sun LY, Hsieh DK, Yu TC, Chiu HT, Lu SF, Luo GH, Kuo TK, Lee OK, Chiou TW. 2009. Effect of pulsed electromagnetic field on the proliferation and differentiation potential of human bone marrow mesenchymal stem cells. Bioelectromagnetics 30(4):251–260.

Tenuzzo B, Chionna A, Panzarini E, Lanubile R, Tarantino P, Di Jeso B, Dwikat M, Dini L. 2006. Biological effects of 6 mT static magnetic fields: A comparative study in different cell types. Bioelectromagnetics 27(7):560–577.

Teodori E, Dei S, Martelli C, Scapecchi S, Gualtieri F. 2006. The functions and structure of ABC transporters: Implications for the design of new inhibitors of Pgp and MRP1 to control multidrug resistance (MDR). Curr Drug Targets 7(7):893–909.

Tewey KM, Rowe TC, Yang L, Halligan BD, Liu LF. 1984. Adriamycin-induced DNA damage mediated by mammalian DNA topoisomerase II. Science 226(4673):466–468.

Tofani S, Barone D, Berardelli M, Berno E, Cintorino M, Foglia L, Ossola P, Ronchetto F, Toso E, Eandi M. 2003. Static and ELF magnetic fields enhance the in vivo anti-tumor efficacy of cis-platin against lewis lung carcinoma, but not of cyclophosphamide against B16 melanotic melanoma. Pharmacol Res 48(1):83–90.

Yang JC, Lee SY, Chen CA, Lin CT, Chen CC, Huang HM. 2010. The role of the calmodulin-dependent pathway in static magnetic field-induced mechanotransduction. Bioelectromagnetics 31(4):255–261.

Zhuang LN, Qi H, Sun RG, Chen WF, Liu Y, Zhu J. 2005. Real time observation on cells in different fixed conditions and living cells in buffer solution by AFM. Acta Biophysica Sinica 21:345–350.